THE JOURNAL OF PHYSICAL CHEMISTRY C

Article

pubs.acs.org/JPCC

Isomerization and Aggregation of the Solar Cell Dye D149

Ahmed El-Zohry, Andreas Orthaber, and Burkhard Zietz*

Department of Chemistry - Ångström Laboratories, Box 523, SE-751 20 Uppsala, Sweden

ABSTRACT: D149, a metal-free indoline dye, is one of the most promising sensitizers for dye-sensitized solar cells (DSSCs) and has shown very high solar energy conversion efficiencies of 9%. Effective electron injection from the excited state is a prerequisite for high efficiencies and is lowered by competing deactivation pathways. Previous investigations have shown surprisingly short-lived excited states for this dye, with maximum lifetime components of 100−720 ps in different solvents and less than 120 ps for surface-adsorbed D149. Using steady-state and time-resolved fluorescence, we have investigated the photochemical properties of D149 in nonpolar and polar solvents, polymer matrices, and adsorbed on ZrO_2, partially including a coadsorbent. In solution, excitation to the S_2 state yields a product that is identified as a photoisomer. The reaction is reversible, and the involved double-bond is identified by NMR spectroscopy. Our results further show that lifetimes of 100−330 ps in the solvents used are increased to more than 2 ns for D149 in polymer matrices and on ZrO_2. This is in part attributed to blocked internal motion due to steric constraint. Conversely, concentration-dependent aggregation leads to a dramatic reduction in lifetimes that can affect solar cell performance. Our results explain the unexpectedly short lifetimes observed previously. We also show that photochemical properties such as lifetimes determined in solution are different from the ones determined on semiconductor surfaces used in solar cells. The obtained mechanistic understanding should help develop design strategies for further improvement of solar cell dyes.

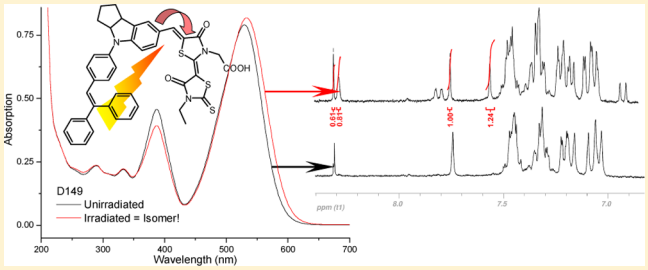

1. INTRODUCTION

Dye-sensitized solar cells (DSSCs) offer a promising, low-cost alternative to silicon solar cells.[1,2] Dyes adsorbed on a mesoporous semiconductor surface, typically TiO_2 or ZnO, absorb light and inject electrons from the excited state into the conduction band of the semiconductor. The dyes are then regenerated by an electrolyte containing a redox-couple. Ru-based dyes have long set the standard for highly efficient DSSCs, but are increasingly replaced by pure-organic, metal free dyes, or compounds containing common transition metals such as zinc. Recently, a zinc porphyrin based, cosensitized DSSC achieved a conversion efficiency of 12.3%.[3] Porphyrins and metal-free organic dyes such as indoline derivatives offer several advantages to Ru-based dyes. They can be produced at lower cost at a large scale, can be used with ZnO, which has shown to be incompatible with many ruthenium complexes[4,5] and, importantly, have higher molar absorption coefficients. The latter is of special importance for solid-state and ionic liquid DSSC, where stringent limits are put on the thickness of the semiconductor. Thinner layers tend not to absorb enough of the incoming light unless dyes with very high absorption coefficients are employed.

Indoline dyes have emerged as a promising class of compounds for DSSC applications. They are synthetically straightforward to obtain and show high photon-to-current efficiency as well as high molar absorption coefficients.[6,7] The central indoline group acts as an electron donating group, stabilized by additional phenyl rings, and is conjugated to an electron accepting group. Cyanoacrylic acid provides accepting properties and acts as a binding group that links to the semiconductor surface. Alternatively, a carboxylic acid coupled to one or more rhodanines has been shown to give intense charge transfer electronic transitions and also high injection yields.[6,7] A time-dependent density functional theory (TD-DFT) study[8] investigating three different candidates of this class confirmed the charge-transfer nature of the $S_0 \rightarrow S_1$ transition, which possesses a very large oscillator strength (f = 2.06) and leads to a dipole moment of >30 D in the excited state.

Also, the frontier orbitals showed the highest occupied molecular orbital (HOMO) to be delocalized over the indoline unit, and the lowest unoccupied molecular orbital (LUMO) to be more localized around the cyanoacrylic acid or rhodanine ring(s). D149 (structure given in Figure 1), one of the most promising of the indoline dyes, has achieved 9.0% light-to-electricity conversion efficiency.[9]

To make best use of the mesoporous surface, tight packing (a monolayer of dye) is desirable for efficient light absorption. This, however, can lead to interaction between nearest neighbors and fundamentally change the photophysical properties of the dye. Aggregation of surface-adsorbed dyes was already observed in the 1970s on cyanine dyes on SnO_2,[10] and later on a range of other systems such as squaraines,[11] phthalocyanines,[12,13] porphyrins,[14] and also on indole-based

Received: July 4, 2012
Revised: November 19, 2012
Published: November 26, 2012

dx.doi.org/10.1021/jp306636w | J. Phys. Chem. C 2012, 116, 26144−26153

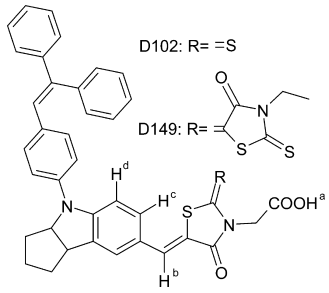

Figure 1. Chemical structure of D102 and D149. Hydrogens with superscript letters are referred to in the NMR-spectra.

donor–acceptor dyes.[9,15] In nearly all cases, aggregation leads to a reduced injection yield and lowers conversion efficiency. Replacement of the ethyl chain of the D149 dye by an octyl chain, aimed at reducing surface aggregation, led to a new compound, D205, that set the record for organic dyes-based solar cells at the time, giving 9.5% conversion efficiency.[16] Interestingly, a coadsorbent (cheno-deoxycholic acid, cDCA) that helps prevent aggregation, was still used to achieve maximum device performance.

Electron injection from the excited state of the surface absorbed dye, a crucial step in solar cell operation, is partially controlled by competing processes that lead to a reduction of the excited state lifetime (such as fast internal conversion or relaxation to lower excitonic states, among others). A thorough knowledge of the dye's photophysics can therefore help optimizing design and conditions of operation. Two previous articles have investigated the excited state properties of D149. Combining pump–probe transient absorption spectroscopy, single photon counting and steady state techniques, the solvent dependence and excited state relaxation was investigated in a wide range of solvents.[17] Solvent relaxation times were found to be subpicosecond to a few picoseconds. Surprisingly, the S_1 lifetime was in the range of 100–800 ps in all solvents investigated, much shorter than the few-nanosecond lifetime expected for a typical organic dye.[18−20] Also, this is considerably shorter than the calculated lifetime for D149 according to TD-DFT calculations where, based on the oscillator strength, a lifetime of τ = 3.2 ns in MeOH was predicted.[8]

Another study used the fluorescence upconversion technique to examine D149 in solution (toluene, acetonitrile), on mesoporous surface (TiO_2 and noninjecting Al_2O_3) and embedded in a polymer matrix (poly(methyl methacrylate), PMMA).[21] While the solution properties largely matched the reported values,[17] very fast deactivation was observed for PMMA and mesoporous films. Electron injection is expected to be fast and will give short lifetimes for TiO_2. However, even on Al_2O_3, the primary decay component (with 60% amplitude) was 2.3 ps, with other components of 16 and 120 ps. For the PMMA embedded D149, 11 ps (41%) and 210 ps (59%) lifetimes were observed. While the fast deactivation on Al_2O_3 is partially explained by aggregation, no reason is given for the fast 210 ps $S_1 \rightarrow S_0$ decay observed in PMMA.

To reconcile D149's very high efficiency as a solar cell sensitizer with the observed short lifetimes in solution and inert media, we have opted to reinvestigate the fluorescence behavior under a range of conditions. Three solvents were chosen—benzene, acetonitrile, and methanol—for their nonpolar, polar, and H-bonding properties, respectively. D149 was also investigated in polar and nonpolar polymer matrices, PMMA and polystyrene (PS). ZrO_2, a high band gap semiconductor, was used to model the photophysics on a noninjecting mesoporous surface with binding properties similar to that of TiO_2.[22] If the short lifetimes observed previously were to be confirmed, we would look to find a mechanistic understanding of the involved photophysical processes. As we will show, double bond isomerization competes with radiative relaxation in solution, reducing the observed lifetimes. Alternatively, if the earlier results could be attributed to effects originating from sample preparation, we would try to optimize the experimental procedure to obtain results that reflect the dye's inherent properties. For solid samples, we will show that aggregation occurs at higher concentrations and leads to fast quenching of the aggregated molecules, and also to quenching of neighboring monomeric molecules by energy transfer.

2. MATERIALS AND METHODS

2.1. Chemicals. D149 was obtained as a kind gift from Masakazu Takata, Mitsubishi Paper Mills, and used as received. Identity and purity, including isomeric purity, were confirmed by means of NMR spectroscopy. The solvents, benzene (Merck, p.a.), acetonitrile and $CHCl_3$ (both Sigma-Aldrich, spectrophotometric grade), MeOH (Sigma-Aldrich, Chromasolve), and tetrahydrofuran (THF) (Riedel de Haën, p.a.) were used without further purification. Plastic fragments of PMMA and PS (ca. 1–5 mm in diameter) were dissolved in $CHCl_3$ and the solution used for doctor blading of polymer films as described below. cDCA (>97%) was used as received from Sigma-Aldrich.

2.2. Steady-State Spectroscopy. Absorption spectra were measured on a Varian Cary 5000, and emission measurements were performed using a Horiba Jobin Yvon Fluorolog and automatically corrected for wavelength dependent instrument sensitivity. Solution measurements where carried out at right angle in a 1 cm cuvette, while films (polymer and ZrO_2) were measured using front face geometry (ca. 30°).

2.3. Time-Correlated Single Photon Counting (TC-SPC). Excitation of the sample was done with a picosecond diode laser (Edinburgh Instruments, EPL405) at 404.6 nm (77.1 ps pulses). The laser's pulse energy was ca. 15 pJ and was attenuated (often more than an order of magnitude) to the desired count rate of ca. 1% or less of the excitation frequency. Specific measurements were performed with 470 nm excitation, but no significant difference in the lifetimes was observed. A cooled (ca. −40 °C) Hamamatsu MCP-photomultiplier R3809U-51 was used for detection of single photons, and the signal passed through a discriminator (Ortec 9307) and into a TAC (Ortec 566, 50 ns range used). The electrical trigger signal from the laser was also passed through a discriminator (Tennelec TC454) and on to the TAC (Ortec 566). The TAC output was read by a DAQ-1 MCA computer card using 8096 channels and collected with Horiba Jobin Yvon DataStation 2.3. Measurements where done in reverse mode at 5 MHz and under magic angle polarization. A cutoff filter, GG475, was used to block stray excitation light. A dilute solution of Ludox was used to record the instrument response function without any filter for solution measurements, while a microscopy glass slide was used to scatter a small part of the excitation for recording the IRF for film measurements. No monochromator was used, i.e., all wavelengths transmitted by the cutoff filter were collected. Dye concentrations were in the range 3–5 μM.

2.4. Streak-Camera Measurements. Excitation of the sample (concentrations between 7 and 10 μM) with ultrafast laser pulses was performed using a frequency-doubled Ti:Sa oscillator (Coherent Mira) output (400 nm) at 76 MHz. Excitation energies at the sample were on the order of 5 pJ (after a CC8 filter to remove residual IR light). A 1 cm cuvette was used, and the laser beam was directed into the cuvette close to the cuvette wall on the emission side, thus reducing the efficient cuvette length to 1−2 mm. Fluorescence at a right angle to the excitation was passed through a Bruker SPEC 250IS spectrograph (ca. 200 nm observation window) and onto the streak camera (Hamamatsu streak camera and blanking unit C5680 in combination with a Synchroscan Unit M5675). The charge-coupled device (CCD) camera (Hamamatsu Orca-ER C4742−95) was used in binning mode (2 × 2 pixels) to give a 512 × 512 pixel matrix. The observed time-windows in different time-ranges were (fwhm instrument response function in parentheses) ca. 160 (5), 800 (20), or 2000 (50) ps.

2.5. NMR Spectroscopy. NMR spectroscopic data were collected with a Varian Mercury+ operating at a proton frequency of 300.03 MHz. ^{1}H spectra of D149 (approximately 1 mg/mL) were recorded in deuterated dimethyl sulfoxide (DMSO-d_6) at 298 K and referenced internally to solvent residual peaks. The isolated singlets between 7.8 and 8.3 ppm corresponding to the olefinic protons exhibited a signal-to-noise ratio of more than 50, which allowed a good estimation of the relative ratios of the two isomers.

2.6. Data Analysis. Decay-curves obtained by single photon counting were analyzed by iterative reconvolution using an exponential decay model with 1, 2, or 3 components in the SpectraSolve Program. For streak camera data, global fits analyzed several wavelengths simultaneously, searching for a global minimum. For streak camera data, a self-written procedure in IgorPro6 was employed assuming a Gaussian instrument response function.

2.7. Polymer Film Preparation (Doctor Blading). To test a highly viscous environment, D149 was embedded in two different polymer matrices. This allows for optical examination of the excited state properties, but limits the large-scale motion of molecules. To obtain a thin film of polymers, the doctor blading technique was employed: a substrate of microscope slides was attached to a horizontal, even surface with tape. The outer edges (ca. 3 mm) of the slides were covered by tape, which served as a spacer of several tens of micrometers. Approximately 100 μL of viscous polymer (PMMA or PS) solution in $CHCl_3$ was added to the lower edge of the slide and quickly and evenly spread over the complete surface with a Pasteur glass pipet and the film dried in vacuo. The films looked even and completely translucent (colored when higher amounts of dye where used). Fluorescence measurements on blank samples were performed to ensure that no background signal due to the polymers was observed.

2.8. ZrO_2 Film Preparation and Sensitization. ZrO_2 paste was prepared according to the procedure described in ref 22. This preparation method had the advantages of giving highly transparent films (estimated particle size ∼12 nm in comparable samples), which strongly reduces scattered light during laser excitation. The paste was doctor-bladed onto microscopy slides and left to dry. Heating of the films was carried out with the following gradient program: heating from 20 to 180 °C (15 min), constant at 180 °C for 10 min, from 180 to 320 °C (15 min), 320 °C for 10 min, heating from 320 to 390 °C (15 min), stable at 390 °C for 10 min, raised from 390 to 450 °C during 15 min, kept at 450 °C for 30 min, and then cooled to 90 °C over 2 h 22 min. Films were sensitized in a solution of D149 (0.5 mM) in THF with varying amounts of cDCA and afterward dried in vacuo.

3. RESULTS AND DISCUSSION

3.1. Steady-State Measurements. To investigate the behavior of the dye D149 in different environments we started by measuring the steady-state absorption and emission properties in three different solvents: nonpolar benzene (C_6H_6, ε_r = 2.2), polar acetonitrile (CH_3CN, ACN ε_r = 36) and protic methanol (CH_3OH, ε_r = 33), which is also able to interact with solutes through hydrogen bonds. The obtained results are shown in Figure 2. The absorption spectra show a

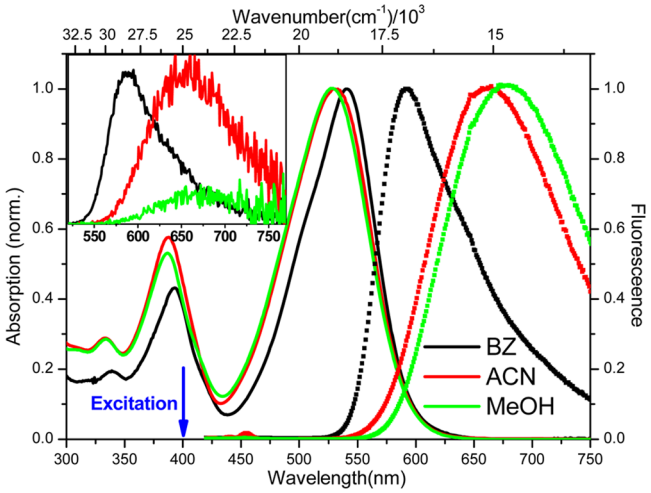

Figure 2. Absorption (solid line) and fluorescence (symbols) spectra of D149 in benzene (black), acetonitrile (green), and methanol (red). The inset shows emission curves normalized to the absorption, i.e., relative quantum yields.

major band centered around 525−550 nm, which has previously been assigned to an intense charge transfer transition based on DFT calculations.[8] The S_2 band is in the near UV (ca. 390 nm) and has been assigned to a $\pi-\pi^*$ transition (mainly LUMO−1→HOMO).[8] A further weak absorption band is discernible around 340 nm.

The emission spectra in benzene show a near-mirror image with a weak vibronic shoulder. Broader and less resolved spectra are observed for the more polar solvents, with a larger Stokes shift of 3140 and 4018 cm^{-1} for acetonitrile and methanol, respectively. The absorption and emission data are summarized in Table 1. As discussed previously,[17] the larger Stokes shift in polar solvents points toward a large dipole moment in the excited state. This is in line with the results from

Table 1. Absorption and Emission Maxima and Stokes Shifts for D149 in the Solvents and Polymer Matrices Investigated

solvent	λ_{max}^{abs} (nm)	λ_{max}^{em} (nm)	$\Delta\tilde{\nu}$ (cm^{-1})
C_6H_6	540	590	1570
CH_3CN	530	661	3740
MeOH	528	670	4015
matrix			
PMMA	533	591	1840
PS	540	605	1990

dx.doi.org/10.1021/jp306636w | J. Phys. Chem. C 2012, 116, 26144−26153

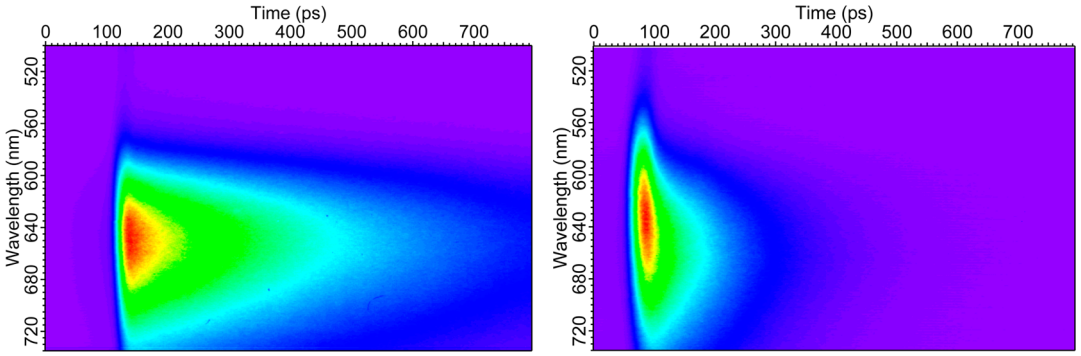

Figure 3. Fluorescence decay for D149 in acetonitrile (left) and in methanol (right). Intensities are normalized, i.e., are not comparable between solvents.

DFT calculations, where μ = 36 D in the excited state compared to μ = 19 D in the electronic ground state.[8]

The inset in Figure 2 shows emission spectra normalized to the absorption at the excitation wavelength, i.e., the areas under these curves are relative quantum yields. It is already clear from the weak signal in methanol that deactivation of D149 is much faster in methanol when compared to the other two solvents. It was appropriate to investigate the kinetics with the help of time-resolved methods.

3.2. Time-Resolved Fluorescence in Solvents. Following excitation of D149 in different solvents with ultrashort laser pulses (λ = 400 nm, few pJ/pulse), we measured time-resolved emission using a streak camera. By analysis of the data with a global fit procedure, we obtained several lifetimes, as none of the measured kinetics could be fitted with a monoexponential model. This is not surprising when taking into account solvent relaxation dynamics. Acetonitrile was chosen to resolve the behavior of D149 in a polar medium. The decay observed is shown in Figure 3. A global fit yielded a short lifetime (1.2 ps, below the time resolution of our equipment) and two medium-long lifetimes of 30 and 330 ps. The longer of these is taken to be the lifetime of the electronic state. The 30 ps component cannot be attributed to solvent relaxation, as the slowest component for acetonitrile is sub-picosecond (630 fs) as determined in a seminal work by the group of Maroncelli.[23] Lohse et al.[17] also found a similar decay component (19 ± 10 ps) for this solvent and a 30 ps time for THF, tentatively assigning it to collisional cooling or structural S_1 relaxation. Also Fakis et al.[21] reported a 23 ± 5 ps decay time for acetonitrile.

In benzene, fitting of the dye's fluorescence resulted in two lifetime components: 25 and 310 ps. The 25 ps component is close to the one mentioned above. It is also practically identical with the slowest of the solvent relaxation times (24.7 ps).[23] However, the latter carries only a small amplitude (3.4% of the relaxation amplitude), while the major amplitude is on the femtosecond time scale and will not reliably show up in our streak camera experiments. Therefore, even for benzene, the component has to be attributed to similar processes as in acetonitrile and THF. The 310 ps lifetime is attributed to the electronic relaxation of D149 in benzene.

The decay of D149 in toluene, which is chemically similar to benzene, had been measured with the upconversion method, and besides a 450 fs rise component, two lifetimes of 40 ± 10 ps (54%) and 630 ± 60 ps (46%) were reported.[21] The faster of these (40 ps) is again comparable to the solvent relaxation in benzene, but has a high amplitude and is likely connected to the 20−30 ps component discussed earlier. The longer, however, is more than twice as large as our result in benzene. To investigate this aspect further, we measured the fluorescence decay in toluene and benzene with single photon counting and streak camera, employing both single wavelength analysis at 600 nm and global analysis, and found lifetimes between 300 and 330 ps (data not shown), very similar to the ones in benzene mentioned above. Although is not fully clear what the difference can be attributed to, at least two aspects might give an explanation: The data measured by upconversion were measured only up to 700 ps. This is too short to reliably fit a 630 ps lifetime, especially as the fit is multiexponential and the component in question carries less than 50% of the amplitude. This aspect has already been pointed out by Lohse et al.[17] for the measurements in acetonitrile. A second rationalization of the different results is that there may be intermolecular interactions between dye molecules in solution that affect relaxation. This aspect has been partially addressed in the work by Fakis, but the lowest concentration investigated was 10 μM (in acetonitrile). We are currently looking at a possible concentration dependence of the lifetimes with single photon counting, a method that allows considerably lower concentration regimes to be investigated. It is noteworthy that for the relatively less polar THF, Lohse et al. found a lifetime of 720 ± 20 ps (besides the 30 ps component discussed earlier). These components are also confirmed in our measurements (data not shown). Therefore, for the nonpolar C_6H_6, a longer lifetime might be expected, based on polarity. Our results show that, besides polarity, additional effects must come into play. Further investigations are currently ongoing in our group.

Due to the presence of several functional groups (such as N, COOH, C═O, C═S), hydrogen bonding may affect the excited state of D149. To specifically test for these effects, we chose to study D149 in methanol solvent, which has comparable dielectric properties to acetonitrile but allows for specific hydrogen bonding. The observed fluorescence decay is seen in Figure 3, where a distinctly nonsymmetric shape is evident. Fitting yields two major lifetimes of 13 and 103 ps and a fast 2.5 ps component. The lifetimes obtained from all fits are also summarized in Table 2. The blue side of the emission shows significantly faster decay, with amplitudes of the ca. 2.5 and 13 ps components dominating. These can be attributed to fast solvent relaxation, including specific H-bonding. A 15.3 ps relaxation was obtained previously for methanol as the longest of the solvent relaxation times,[23] while the faster components are not fully resolved in our measurements. Interestingly, however, the major component related to the electronic

dx.doi.org/10.1021/jp306636w | J. Phys. Chem. C 2012, 116, 26144−26153

Table 2. Lifetimes Obtained from Global Fits of S_1 for D149 in Different Solvents[a]

solvent	τ_1/ps (A_1)	τ_2/ps (A_2)	τ_3/ps (A_3)
C_6H_6		25 (37%)	310 (63%)
MeCN	1.2 (52%)	30 (7%)	330 (41%)
MeOH	2.5 (27%)	13.2 (38%)	103 (35%)

[a]Amplitudes are given for the emission maximum.

excitation (103 ps) is substantially shorter compared to acetonitrile (330 ps), in spite of the similar solvent polarity. This effect has already been described by Lohse et al.,[17] who found a faster decay (178 ps) for ethanol, despite being less a polar solvent compared to acetonitrile.

3.3. Fluorescence Properties in Polymer Matrix. From the new time-resolved fluorescence data and previous work, it can be concluded that the excited state lifetimes of D149 in a wide range of solvents are on the order of 100s of ps and that lifetimes are further reduced by protic solvents. While the specific effect of hydrogen bonding deserves further attention and is currently under investigation in our group, we note that even in aprotic solvents (polar and nonpolar), short lifetimes are observed.

Concerning the mechanistic details of deactivation, it is important to note that D149 contains three exocyclic double-bonds. Twisting of double bonds in the excited state is a very well-known mechanism for fast deactivation, with great relevance in biological processes, such as light detection by retinal in the visual protein rhodopsin[24] or phototherapy of neonatal jaundice.[25] Many of the observed reactions happen on a very fast time-scale, hundreds of femtoseconds to a few picoseconds. In the case of stilbene, for example, a barrierless excited state reaction is observed with time constants of ca. 1 ps, varying with solvent viscosity.[26] For the photoreaction of thermodynamically more stable *trans*-stilbene, an excited state barrier is assumed to slow down the reaction and increase the time constant to ca. 80 ps.[27] Besides leading to a lower rate constant for *trans*-stilbene, a temperature dependence is also observed following the Arrhenius equation. In another example, efficiencies of DSSCs based on the triphenylamine dye NK7 were reduced compared to those using amines with methyl side chains (NK1 and NK2). This was explained, at least in part, by the excited state rotation of the phenyl groups competing with electron injection.[28] The time scale for this isomerization-like behavior was assigned to tens to hundreds of femtoseconds.

Rotation around the double bond lowers the excited state energy while at the same time increasing the ground state energy, often leading to a touching of surfaces (conical intersection), thereby allowing the molecule to pass efficiently to the ground state. A conical intersection has, for instance, been shown for a bilirubin model, explaining the fast lifetimes observed in the processes relevant for phototherapy of neonatal jaundice.[29] The exact potential energy landscape determines the quantum yield, in some cases allowing molecules to deactivate without forming a photoproduct (isomer). To test whether large-scale intramolecular motions are involved in the deactivation, we sought to restrict rotational freedom of D149 and chose to embed the dye in solid plastic matrices. PMMA, containing ester groups, and aromatic PS were chosen as transparent media with polar and nonpolar properties, respectively.

The results for time-resolved fluorescence measured by the TC-SPC method are given in Figure 4, with the obtained fitting parameters given in Table 3. Laser pulses of 405 nm with pulse energy less than 4 pJ were used to excite the sample. Clearly,

Table 3. Lifetimes obtained by TC-SPC of D149 in plastic matrices and on ZrO_2 films with varying amounts of cDCA as co-adsorbent. Also given are quantum yields relative to D149/ZrO_2/40 mM cDCA, calculated from the lifetimes

matrix	τ_1/ps (A_1)	τ/ps (A_2)	
PMMA	1200 (35%)	2550 (65%)	
PS	1200 (40%)	2320 (60%)	
ZrO_2 + x mM cDCA			rel. Φ
0	440 (70%)	1800 (30%)	0.56
1	500 (65%)	1900 (35%)	0.66
10	600 (55%)	1960 (45%)	0.81
40	700 (50%)	2300 (50%)	1

lifetimes increase considerably compared to solution and are not very sensitive to the polar versus nonpolar environment. Of the two lifetime components, the longer one is likely to be close to the natural lifetime. Le Baher et al.[8] have estimated the expected lifetime based on the oscillator strength and calculated fluorescence energy, according to the Einstein transition probability formula. The obtained value of 3.23 ns is longer than our longer value, but it is not clear whether the difference is due to other remaining deactivation processes in the experimental value or due to approximations for obtaining the theoretical value. In any case, a nearly 10-fold increase in fluorescence lifetimes compared to solution shows that the major deactivation path acting in solution is blocked in the matrix for the longer component, while a second decay channel still exists and keeps lifetimes of 1.2 ns for a subpopulation of molecules.

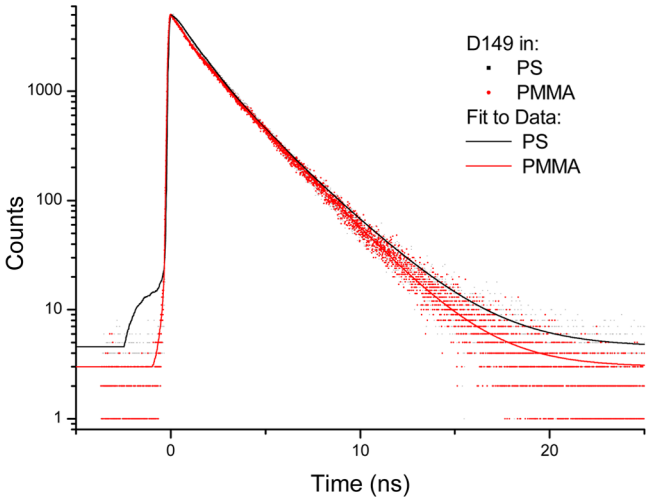

Figure 4. Fluorescence decay of D149 in PS (black) and PMMA (red) after excitation at 405 nm.

The results from Figure 4 were obtained for dilute samples (ca. 400 μM, corresponding to OD = 0.05). Increasing the concentration of D149 by a factor of 4 led to an important change: a short-lived component visible on the blue side of the emission spectrum appears (Figure 5). The new fast (few-ps) decay is likely to occur due to aggregation of D149 within the matrix. It is probable that this species was observed by Fakis et

dx.doi.org/10.1021/jp306636w | J. Phys. Chem. C 2012, 116, 26144–26153

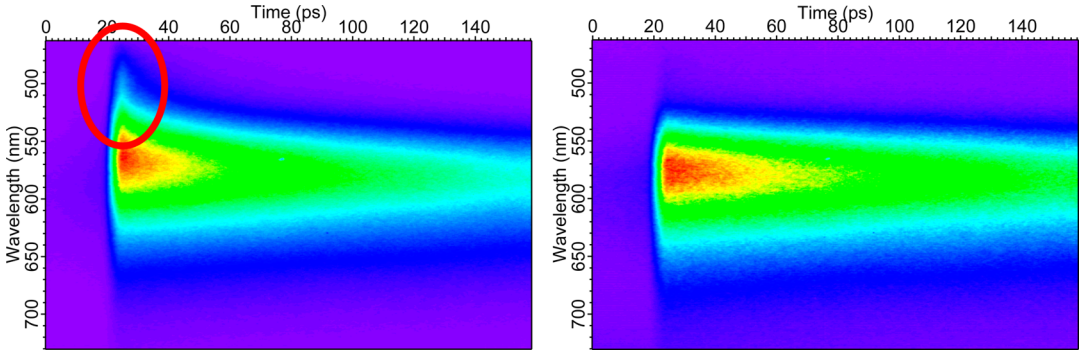

Figure 5. Fluorescence decay in a concentrated (left) and dilute (right) D149/PMMA matrix.

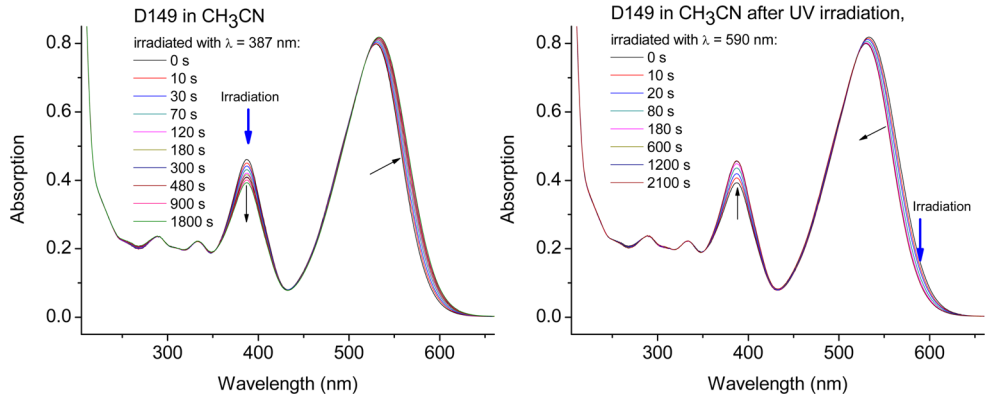

Figure 6. Absorption spectra of D149 in CH_3CN after irradiation with UV light (left) and with visible light after UV irradiation (right).

al.,[21] explaining their fast decay times of 11 and 210 ps. The precise lifetimes will then be dependent on the exact degree of aggregation and are expected to vary from sample to sample.

3.4. Isomerization. Seeing a large increase in the excited state lifetimes of D149 in a rigid environment points toward a large-scale twisting motion as the relaxation pathway. Thus it would be of value to identify any possible photoproducts that may have formed as a result of isomerization. Isomers of similar dyes have been calculated by DFT previously.[30] Upon irradiation of a solution of D149 in acetonitrile with UV light (387 nm, maximum of the S_2 band), the absorption spectrum changes in two ways: a shift and broadening of the S_1 band, and a decrease in intensity of the S_2 band (Figure 6). A change of the absorption spectrum after irradiation with UV light and a photostationary state was previously observed, but not examined in detail.[17] The light-induced changes can be reversed upon illumination with visible light (590 nm), proving that a reversible photoisomerisation is taking place, and that the molecule is not chemically transformed by, e.g., photo-oxidation.

As D149 contains three exocyclic double bonds, it is not obvious which of these is involved in the formation of a photoproduct. From a symmetry argument, isomerization of the diphenyl-vinyl double bond will not lead to a photoproduct different from the thermodynamic isomer and can be excluded. To further differentiate between the two remaining double bonds, we have used D102 for comparison. Here, only one rhodanine group is present (see Figure 1 for structure). Irradiation into the S_2 band was performed in a similar way as for D149, and a similar, but smaller red shift in the absorption spectrum could be seen (data not shown). Also in this case, a recovery of the initial isomeric form was observed when irradiated with visible light. As D102 only has one double bond that can lead to a photoisomer, we can already conclude that rotation around the C═C linkage connecting the rhodanine and phenyl ring is involved in the isomerization.

^{1}H NMR spectroscopy was used to further elucidate this point. D149 was dissolved in DMSO-d_6 and split in two equal samples: one was irradiated at 400 nm under stirring until a photostationary state was reached, while the other sample was kept in the dark. The region from 6.8 ppm to 8.4 ppm of the recorded spectra is depicted in Figure 7. As reported earlier,[7] D149 shows a large number of unresolved aromatic and olefinic signals between 7.0 and 7.5 ppm. Two resolved singlets of

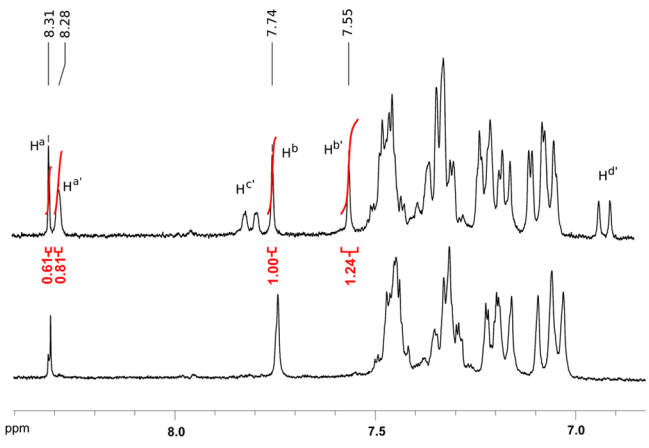

Figure 7. ^{1}H-NMR spectrum of irradiated (λ = 400 nm, top) and unirradiated (bottom) D149 in DMSO-d_6; H^a–H^d refer to the protons given in Figure 1, their primed form $H^{a'}$-$H^{d'}$ to the isomerized form.

dx.doi.org/10.1021/jp306636w | J. Phys. Chem. C 2012, 116, 26144–26153

approximately 1H integral at 7.73 and 8.31 ppm can be attributed due to their chemical shift and multiplicity (no coupling) to the proton (H^b in Figure 1) in the vinyl group bridging the rhodanine and the phenyl unit and the acidic proton (H^a), respectively. Exchange with residual water slightly lowers the acidic proton integral signal. In the irradiated sample, new singlets appear at ca. 7.53 and 8.29 ppm. Due to the large shift ($\Delta\delta_H$ = 0.2 ppm) from 7.73 to ca. 7.53 ppm, this signal can be attributed to the hydrogen attached to the isomerising bond (H^b), whereas the carboxylic acid is hardly effected ($\Delta\delta_H$ = 0.02 ppm). Two additional doublets at 6.91 and 7.80 ($^3J_{HH}$ 8.5 Hz) can be further discriminated in the aromatic region, which are assigned to the *meta* (H^d) and *ortho* (H^c) protons of the phenyl ring adjacent to the isomerising double bond, respectively. These newly appearing doublets were previously hidden in the unresolved aromatic region between ca. 7.00 and 7.50 ppm, and their large change in chemical shift originates from the significant change of environment in the isomerized species. These findings confirm that the isomerization can be assigned to the C═C double bond linking the rhodanine moiety and the phenyl group.

Integration of the isolated singlets of both the isomerized and unisomerised form gives an estimate of the ratio of the two species in the irradiated sample, yielding a ratio of ca. 55% of photoisomerized to 45% of nonisomerized form. This in turn allows for the calculation of the absorption spectrum of the pure photoisomer. We assume isomerically pure starting material (as shown by NMR) with an absorption $A(\lambda) = A_{D149}$. As indicated by the isosbestic points, irradiation leads to exactly one photoproduct, isomD149. The mixed sample's absorption consists thus of two contributions:

$$A_{mix} = x \cdot A_{D149} + y \cdot A_{isomD149}$$

Knowing the mole fraction x and y corresponding to the amount of photoconversion from the NMR data ($x + y = 1$), we can solve for the absorption of the pure isomerized form:

$$A_{isomD149} = (A_{mix} - x \cdot A_{D149})/y$$

Accordingly, from the absorption sample of the mixture, the fraction of nonisomerized absorption was subtracted and the spectrum normalized. The result gives an approximated UV–vis absorption spectrum of the pure photoisomer, as can be seen in Figure 8. The absorption maximum in the S_1-band is located at 537 nm, a 7 nm (246 cm^{-1}) shift compared to D149.

The large difference in excited state lifetimes in different solvents ranging from 100 ps in methanol to >700 ps in THF cannot be explained by a simple excited state reaction depending only on, e.g., solvent viscosity or polarity. Protic media show a reduction of lifetime that is separate from the effects of polarity. Also, as mentioned above, a concentration dependence of lifetimes is observed in some solvents. From this it becomes clear that several processes besides isomerization are contributing to the nonradiative rates. For the samples in PMMA and PS, however, all of the competing reactions can be excluded for the major part of the population, giving the natural lifetime with a large amplitude. It is thus at the moment not possible to attribute a single time constant to the isomerization process, but it is becoming clear that a thermal barrier is involved, as a barrierless reaction would happen on a femtosecond–picosecond time scale and outcompete other side reactions. We have tested for the possibility of a barrier in the excited state by measuring lifetimes of D149 in acetonitrile at different temperatures (5 to 60 °C) and see a clear increase in rates with higher temperature (data not shown).

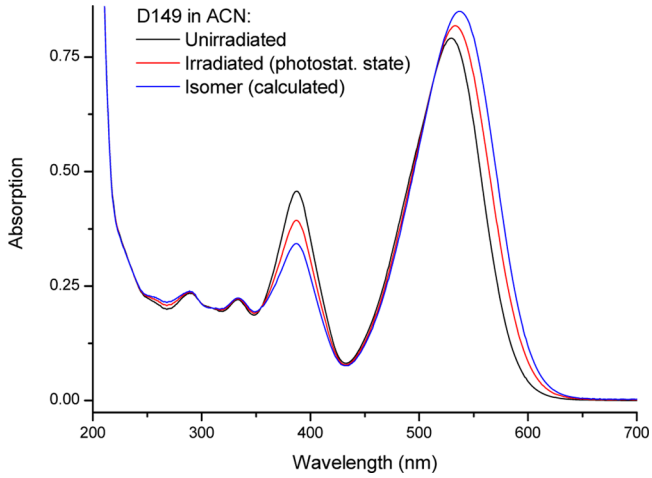

Figure 8. Absorption spectra of unirradiated D149 (black curve), D149 in the photostationary state (red) and the calculated, normalized absorption spectrum of the pure photoisomer (blue).

3.5. Behavior on Semiconductor Surface. D149 has been developed for solar cell applications. In order to find out if any of the above-mentioned deactivation processes are relevant on the surface of a semiconductor, we chose to investigate the photophysical behavior of D149 adsorbed to a film of mesoporous zirconium oxide. ZrO_2 is a high-band gap semiconductor that allows similar anchoring of sensitizers as TiO_2, but prevents electron injection due to the high-lying conduction band.[31,32] This enabled us to study purely photophysical processes independent of electron injection that could be taking place when using TiO_2. The previous upconversion study[21] of D149 had shown very short lifetimes on Al_2O_3 (another high-band gap semiconductor), but these may have been affected by aggregation, similar to the polymer matrix sample. We used different concentrations of the additive cDCA as coadsorbent to minimize dye molecule aggregation. At the same time, however, the amount of dye that can be loaded onto a given surface is reduced and therefore leads to lowered light-harvesting efficiencies.

Steady-state fluorescence spectra of D149 adsorbed to ZrO_2 are seen in Figure 9. While showing a roughly similar shape, they are systematically shifted to shorter wavelengths with higher concentration of coadsorbent. Put differently, increasing the concentration of (and thus reducing the distance between) D149 molecules leads to a red-shift. Two main factors are likely to contribute to this effect. First, relaxation of the environment can lower the energy of the excited state, leading to a red-shifted emission as is observed in MeOH and acetonitrile. The surrounding cDCA would in this case behave like a nonpolar environment, with D149 itself being more polar and allowing for relaxation to lower energy. A second and more plausible reason is long-range energy transfer between D149 molecules with different microenvironments, which leads to trapping of energy at the lowest site within the transfer radius. As can be seen in the inset of Figure 9, the emission of D149 without cDCA corresponds to the red-most part of the emission band of D149 in the presence of cDCA. Also apparent is the reduction in intensity, which is in line with nonquantitative energy transfer, i.e., the loss of energy at each transfer step. Because quantum yields are difficult to measure on films that

dx.doi.org/10.1021/jp306636w | J. Phys. Chem. C 2012, 116, 26144–26153

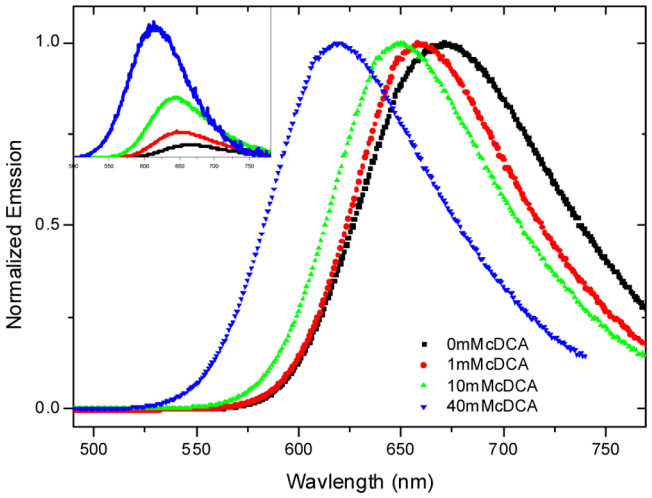

Figure 9. Steady-state fluorescence spectra of D149 on ZrO_2 with different amounts of cDCA as coadsorbent. The inset shows spectra normalized to the number of absorbed photons, i.e. relative quantum yield.

are mesoporous (and thus highly scattering) and often also macroscopically heterogeneous, we performed TC-SPC experiments on each sample. This technique has the advantage of being independent of (absolute) fluorescence intensity. The decay curves of four samples with varying cDCA content, together with the instrument response function, are seen in Figure 10. The lifetimes obtained from biexponential fits are

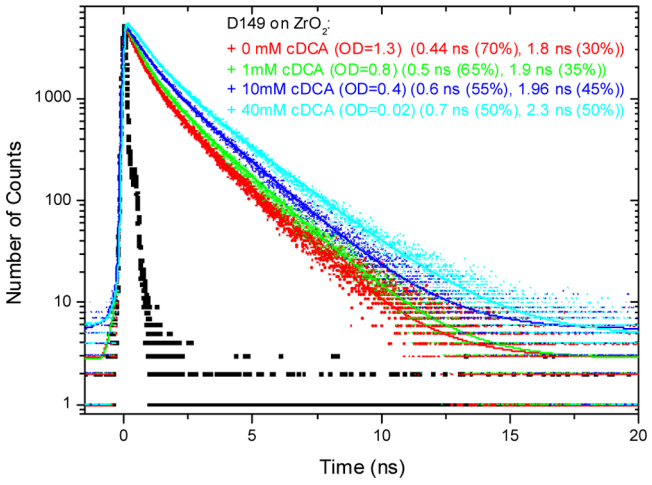

Figure 10. Time-resolved fluorescence (TC-SPC) of D149 on ZrO_2 with various amounts of cDCA. The black, dotted line represents the instrument response function.

also given in Figure 10 and in addition summarized in Table 3. Here, we have also calculated quantum yields relative to the 40 mM cDCA sample, based on the lifetimes and amplitude. As expected from the steady-state emission measurements, using higher concentrations of cDCA leads to longer lifetimes and thus higher quantum yields. In the case of high cDCA concentration (40 mM), the longer component (>2 ns) is similar to the longest component observed in PMMA and PS matrix. For the other samples containing less cDCA, energy transfer processes reduce the corresponding lifetime. It is noteworthy that the maximum amount of cDCA used corresponds to an 80-fold excess in concentration relative to the sensitizer. This also leads to a severe decrease of adsorbed dye and thus strongly reduced light-harvesting efficiency. Still, such high concentrations of coadsorbent are needed to reach lifetimes comparable to the natural lifetime. While electron injection is much faster than fluorescence and can compete more efficiently with other processes such as energy transfer, it is obvious that coadsorbers are not the best way of preventing aggregation. Instead of wasting precious surface area with inactive molecules, the long-term strategy should be to design molecules that are less prone to aggregation.

In all ZrO_2 samples, a second lifetime component is present that could be attributed to isomerization of surface-bound molecules that have enough steric freedom to allow large scale rotation. It should be noted that a reduction of excited state lifetime does not require for the isomerization mechanism, i.e., double bond twisting, to form a photoproduct. A partial twisting, as can occur in somewhat restricted environment, could also lead to deactivation of the excited state.

3.6. Implications for DSSCs. *Isomerization.* DSSCs rely on efficient electron injection from the excited state of the absorbing dye into the semiconductor layer. In order for this crucial step to be efficient, competitive processes need to be slow in comparison. Electron injection has frequently been assumed to be happening on the time-scale of ca. 100 fs, based on measurements of dyes adsorbed onto TiO_2.[33,34] These measurements were often performed in the absence of electrolyte and using laser intensities that far exceed normal operating conditions of ca. one sun (AM = 1.5). On the basis of an injection rate of $(100\ fs)^{-1}$ and using 300 ps as the lifetime of D149 in fluid solution taken as the sum of competitive processes, the corresponding efficiencies would exceed 99.96% and could be safely ignored. However, recent experiments show hundreds of femtoseconds to a few picoseconds injection times for surface-adsorbed N3 dye in the absence of electrolyte, increasing to hundreds of picoseconds when an electrolyte is present with 50% of injection occurring with ca. 500 ps.[35] We are not aware of any comparable measurement for metal-free dyes in the presence of electrolyte and with low excitation energy. The behavior can possibly be attributed to Ru-dyes specifically, although aspects such as excitation laser power and repetition rate are still likely to be relevant for pure organic dyes. For D149, the maximum incident photon-to-current efficiency (IPCE) is around 95%.[9] As the IPCE includes injection and regeneration efficiency, isomerization as a competitive process can in this case account for at most 5%, (or less in the case of regeneration efficiency <100%). However, isomerization can have larger importance for other dyes and has hitherto not been taken into consideration.

In order to achieve the highest possible open circuit voltage, the design of the dye-semiconductor couple should be such that the conduction band is relatively close to the LUMO level of the injecting dye. As a consequence, the driving force will be lowered and electron injection slowed down. This gives further reason to reduce competitive processes as much as possible.

The effects of photoisomerisation on the performance of the DSSC are not limited to the reaction itself. Also the reaction product, the photoisomerised dye, needs to be taken into account. At the moment, it is unclear whether the photoproduct has comparable properties as sensitizer and will inject and regenerate with similar efficiency. Ning et al. report a reduced efficiency of a dye (S1) in its Z-form (3.72% vs 5.77% in the E-form).[36] This is explained by the geometric arrangement of the dye on the surface: the electron donating

dx.doi.org/10.1021/jp306636w | J. Phys. Chem. C 2012, 116, 26144−26153

part of the molecule is close to the TiO_2 in the Z-form, whereas the larger distance maintained in the E-form prevents recombination between the electron in the TiO_2 and the positive donor group of the molecule.

While it is not clear at the moment to what extent isomerization processes occur on the semiconductor surfaces, it is not the only competitive pathway for excited molecules. Large-scale motion under isomerization of D149 moieties can also lead to a disruption of molecular order of the surface-adsorbed dyes. This could allow for increased contact between TiO_2 and electrolyte and open a channel for recombination of injected electrons with the electrolyte. Here, even a small quantum yield of isomerization could have a detrimental effect due to the lost surface coverage.

In one of the few studies investigating the effects of isomerization of solar cell dyes, Lin et al.[20] have looked at a triphenylamine-stilbene system that isomerizes under the influence of light. In a comparative molecule, the stilbene double bond was incorporated into a five-membered ring, preventing isomerization. An improvement of ca. 13% in efficiency was observed, ranging from 4.52 to 4.98% for different isomerizing systems, compared to 5.14 to 5.67% for corresponding locked variants. Interestingly, lifetimes reported for the systems undergoing photoisomerisation in an aprotic solvent (2.12−2.52 ns) were not much shorter than the ones for the nonisomerising systems (2.43−2.95 ns). For D149, lifetimes in aprotic solvents are reduced more dramatically to hundreds of picoseconds, compared to ca. 2.5 ns for D149 in polymer. Preventing isomerization in a structurally modified D149 derivative could thus have a larger, positive impact on D149 efficiencies when compared to the stilbene systems.

Aggregation. The existence of an additional, short lifetime component of concentrated samples of D149 in polymer matrices shows that a new pathway, competing with electron injection, is opened if molecules get in close contact. While the phenomenon is less pronounced on a mesoporous surface (as ZrO_2), a reduction of lifetimes is still visible, with a further component of energy transfer emerging. The latter is of less concern as the associated rates of less than $\sim 1\ ns^{-1}$ are much smaller than the direct quenching due to aggregation (few ps^{-1}). The most efficient solar cell devices based on D149 and similar dyes have relied on the addition of cDCA as coadsorbent to separate molecules efficiently[16] and an increase in efficiency of 7% (for D149) and 11% (D205) was observed, showing that aggregate formation has direct consequences on the performance of working solar cells, confirming the trend seen in our fluorescence measurements. While the approach of adding coadsorbent is feasible, it reduces the amount of dye that can be placed onto the semiconductor, and thereby reduces precious surface space and the light-harvesting efficiency. A promising approach to separate molecules while keeping tight coverage is the addition of long-chain side groups. This approach has been chosen in the dyes D205 and D358 and has let to improved efficiencies of up to 9.5% for D205.[16] We are currently studying these new molecules to see whether the modifications are reflected in longer excited state lifetimes due to reduced aggregation.

4. CONCLUSIONS

Excited state life times for the sensitizer D149 have been measured and compared to previous results. The relatively fast deactivation in solution (100 ps in H-bonding, polar solvents to ca. 700 ps in nonpolar solvents) is confirmed and explained by, among others, a large-scale molecular motion of D149. Incorporation of D149 in a solid polymer matrix leads to a large increase in lifetimes, approaching the natural lifetime (>2 ns). Very fast deactivation (fs to few ps range) can be explained by aggregation and is the likely reason for fast decays observed earlier, with more dilute samples showing longer lifetimes. The effect of aggregation is seen both in polymer matrix and on ZrO_2, having severe consequences for the electron injection by competitive deactivation.

Investigation of the photoproduct of irradiation into the S_2 band revealed that isomerization around an exocyclic double bond is a further deactivation mechanism. The position of the isomerising double bond, and thus the structure of the photoisomer, is resolved by NMR spectroscopy. Structural modifications to avoid the detrimental effects of aggregation and isomerization, for example competition with electron injection and disruption of surface order, can hopefully lead to a further improvement in efficiencies for this class of molecules.

AUTHOR INFORMATION

Corresponding Author

*E-mail: burkhard.zietz@kemi.uu.se.

Notes

The authors declare no competing financial interest.

ACKNOWLEDGMENTS

We would like to thank Masakazu Takata for kindly sending a sample of D149 and D102. A.O. is grateful to the Austrian Science Fund (FWF) for an Erwin-Schrödinger fellowship (J 3193). We also express thanks to S. Glover for proofreading the manuscript.

REFERENCES

(1) Hagfeldt, A.; Boschloo, G.; Sun, L. C.; Kloo, L.; Pettersson, H. *Chem. Rev.* **2010**, *110*, 6595.
(2) O'Regan, B.; Grätzel, M. *Nature* **1991**, *353*, 737.
(3) Yella, A.; Lee, H. W.; Tsao, H. N.; Yi, C. Y.; Chandiran, A. K.; Nazeeruddin, M. K.; Diau, E. W. G.; Yeh, C. Y.; Zakeeruddin, S. M.; Grätzel, M. *Science* **2011**, *334*, 629.
(4) Yoshida, T.; Zhang, J.; Komatsu, D.; Sawatani, S.; Minoura, H.; Pauporté, T.; Lincot, D.; Oekermann, T.; Schlettwein, D.; Tada, H.; Wöhrle, D.; Funabiki, K.; Matsui, M.; Miura, H.; Yanagi, H. *Adv. Funct. Mater.* **2009**, *19*, 17.
(5) Keis, K.; Lindgren, J.; Lindquist, S.-E.; Hagfeldt, A. *Langmuir* **2000**, *16*, 4688.
(6) Horiuchi, T.; Miura, H.; Uchida, S. *Chem. Commun.* **2003**, 3036.
(7) Horiuchi, T.; Miura, H.; Sumioka, K.; Uchida, S. *J. Am. Chem. Soc.* **2004**, *126*, 12218.
(8) Le Bahers, T.; Pauporte, T.; Scalmani, G.; Adamo, C.; Ciofini, I. *Phys. Chem. Chem. Phys.* **2009**, *11*, 11276.
(9) Ito, S.; Zakeeruddin, S. M.; Humphry-Baker, R.; Liska, P.; Charvet, R.; Comte, P.; Nazeeruddin, M. K.; Pechy, P.; Takata, M.; Miura, H.; Uchida, S.; Grätzel, M. *Adv. Mater.* **2006**, *18*, 1202.
(10) Memming, R. *Faraday Discuss.* **1974**, *58*, 261.
(11) Geiger, T.; Kuster, S.; Yum, J. H.; Moon, S. J.; Nazeeruddin, M. K.; Grätzel, M.; Nüesch, F. *Adv. Funct. Mater.* **2009**, *19*, 2720.
(12) Deng, H. H.; Mao, H. F.; Liang, B. J.; Shen, Y. C.; Lu, Z. H.; Xu, H. J. *J. Photochem. Photobiol., A* **1996**, *99*, 71.
(13) Humphry-Baker, N.; Driscoll, K.; Rao, A.; Torres, T.; Snaith, H. J.; Friend, R. H. *Nano Lett.* **2012**, *12*, 634.
(14) Mikroyannidis, J. A.; Charalambidis, G.; Coutsolelos, A. G.; Balraju, P.; Sharma, G. D. *J. Power Sources* **2011**, *196*, 6622.
(15) Horiuchi, T.; Miura, H.; Uchida, S. *J. Photochem. Photobiol., A* **2004**, *164*, 29.

(16) Ito, S.; Miura, H.; Uchida, S.; Takata, M.; Sumioka, K.; Liska, P.; Comte, P.; Pechy, P.; Grätzel, M. *Chem. Commun.* **2008**, *2008*, 5194.
(17) Lohse, P. W.; Kuhnt, J.; Druzhinin, S. I.; Scholz, M.; Ekimova, M.; Oekermann, T.; Lenzer, T.; Oum, K. *Phys. Chem. Chem. Phys.* **2011**, *13*, 19632.
(18) Lakowicz, J. R. *Principles of Fluorescence Spectroscopy*, 3rd ed.; Springer: New York, 2006.
(19) Turro, N. J.; Ramamutrhy, V.; Scaiano, J. C. *Principles of Molecular Photochemistry - An Introduction*; Universiy Science Books: Sausalito, CA, 2009.
(20) Lin, Y.-D.; Chow, T. J. *J. Mater. Chem.* **2011**, *21*, 14907.
(21) Fakis, M.; Stathatos, E.; Tsigaridas, G.; Giannetas, V.; Persephonis, P. *J. Phys. Chem. C* **2011**, *115*, 13429.
(22) Thyagarajan, S.; Galoppini, E.; Persson, P.; Giaimuccio, J. M.; Meyer, G. J. *Langmuir* **2009**, *25*, 9219.
(23) Horng, M. L.; Gardecki, J. A.; Papazyan, A.; Maroncelli, M. *J. Phys. Chem.* **1995**, *99*, 17311.
(24) Sundström, V. *Prog. Quantum Electron.* **2000**, *24*, 187.
(25) Zietz, B.; Gillbro, T. *J. Phys. Chem. B* **2007**, *111*, 11997.
(26) Todd, D. C.; Jean, J. M.; Rosenthal, S. J.; Ruggiero, A. J.; Yang, D.; Fleming, G. R. *J. Chem. Phys.* **1990**, *93*, 8658.
(27) Courtney, S. H.; Fleming, G. R. *J. Chem. Phys.* **1985**, *83*, 215.
(28) Myllyperkiö, P.; Manzoni, C.; Polli, D.; Cerullo, G.; Korppi-Tommola, J. *J. Phys. Chem. C* **2009**, *113*, 13985.
(29) Zietz, B.; Blomgren, F. *Chem. Phys. Lett.* **2006**, *420*, 556.
(30) Matsui, M.; Ito, A.; Kotani, M.; Kubota, Y.; Funabiki, K.; Jin, J.; Yoshida, T.; Minoura, H.; Miura, H. *Dyes Pigm.* **2009**, *80*, 233.
(31) Moser, J.-E.; Wolf, M.; Lenzmann, F.; Grätzel, M. *Z. Phys. Chem.* **1999**, *212*, 85.
(32) Kalyanasundaram, K.; Grätzel, M. *Coord. Chem. Rev.* **1998**, *177*, 347.
(33) Kar, P.; Banerjee, T.; Verma, S.; Sen, A.; Das, A.; Ganguly, B.; Ghosh, H. N. *Phys. Chem. Chem. Phys.* **2012**, *14*, 8192.
(34) Kuang, D.; Ito, S.; Wenger, B.; Klein, C.; Moser, J.-E.; Humphry-Baker, R.; Zakeeruddin, S. M.; Grätzel, M. *J. Am. Chem. Soc.* **2006**, *128*, 4146.
(35) Juozapavicius, M.; O'Regan, B. C.; Kaucikas, M.; Thor, J. J. v. Picosecond electron injection in optimised dye-sensitised solar cells with visible pump mid-infrared-probe transient absorption spectroscopy. *4th International Conference on Hybrid and Organic Photovoltaics*, 2012, Uppsala, Sweden.
(36) Ning, Z.; Fu, Y.; Tian, H. *Energy Environ. Sci.* **2010**, *3*, 1170.